ACS APPLIED MATERIALS & INTERFACES

Research Article

www.acsami.org

Molecular Design for Moisture Insensitivity of Compositionally Graded Hybrid Films

Marta Giachino,[†] Geraud Dubois,*[,†,‡] and Reinhold H. Dauskardt*[,†]

[†]Department of Materials Science and Engineering, Stanford University, Stanford, California 94305, United States

[‡]Hybrid Polymeric Materials, IBM Almaden Research Center, 650 Harry Road, San Jose, California 95120, United States

ABSTRACT: Effective bonding of organic/inorganic interfaces especially in high humidity environments is paramount to the structural reliability of modern multilayer device technologies, such as flexible electronics, photovoltaics, microelectronic devices, and fiber-metal laminates used in aerospace applications. We demonstrate the ability to design compositionally graded hybrid organic/inorganic films with an inorganic zirconium network capable of forming a moisture-insensitive bond at the interface between an oxide and organic material. By controlling the chemistry of the deposited films and utilizing time-dependent debonding studies, we were able to correlate the behavior of the hybrid films at high humidity to their underlying molecular structure. As a result, an outstanding threefold improvement in adhesion of silicon/epoxy interfaces can be obtained with the introduction of these films even in high humidity environments.

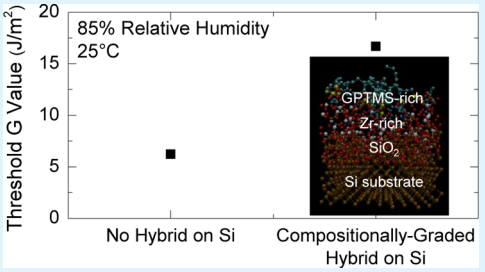

KEYWORDS: *hybrid materials, thin films, organic/inorganic interfaces, moisture insensitivity, sol–gel*

1. INTRODUCTION

Organic/inorganic interfaces that contain reactive atomic bonds are often weak in the presence of reactive environmental species, such as moisture, leading to interfacial debonding and poor reliability of multilayer devices and laminates.[1−9] Hybrid molecular materials that contain bonds that are resistant to such environmental species can be synthesized via sol–gel chemistry and uniquely tailored to address these challenges.[10−16] The intimate nanometer length-scale mixing of their organic and inorganic components allows the design of molecular networks that are capable of mitigating the detrimental effects of reactive species by inhibiting diffusion through the material and presenting bonds insensitive to attack.

We recently reported on an adhesive hybrid organic/inorganic system synthesized using an epoxy-functionalized silane, (3-glycidoxypropyl)trimethoxysilane (GPTMS), and an acetate-stabilized zirconium alkoxide, tetra-*n*-propoxyzirconium (TPOZ-Ac).[14,15,17−20] The optimal molecular structure was obtained using sol–gel chemistry and by tuning the sol–gel processing parameters.[15] Here, we explore the adhesive and cohesive properties of the films in both inert and reactive humid environments. We specifically control the hydrolysis and condensation reactions of the zirconium precursor to understand the role of the moisture-insensitive network on the moisture-assisted degradation. As a result, we designed hybrid organic/inorganic films that improve the adhesion by at least threefold, even in high humidity environments.

We utilized a well-established thin-film mechanical testing technique to measure the adhesion and cohesion of the films, where the critical fracture energy G_c (J/m^2) can be quantified in terms of the energy per unit area required to propagate a crack through a single material or interface.[14,15,21] However, G_c alone does not provide any information regarding the debonding kinetics and the sensitivity of the hybrid films to the environment; therefore, it should be coupled with time-dependent debonding studies.[3,21−24] The importance of these measurements in designing hybrid films for resistance to chemically reactive environments is highlighted in this study. While G_c values of the films with optimal graded structures were elevated by as much as 10-fold, the time-dependent debonding converged to much lower threshold G values. Nevertheless, the threshold G values for the hybrid films measured at high humidity were threefold the threshold value in the absence of the adhesive films, suggesting that these hybrids dramatically improve the resistance of epoxy/Si interfaces to moisture-assisted degradation.

The behavior of these films to time-dependent debonding was found to be a function of the underlying molecular structure of the films, which is a direct result of the sol–gel reaction parameters. We prehydrolyzed TPOZ-Ac in an excess of water for varying time, followed by the addition of GPTMS to the solution, which was aged for 5 min, and dip coated onto natively oxidized Si substrates.[15] Dilute solution conditions (3.75 wt %) were used to slow down the kinetics of the hydrolysis and condensation reactions of the TPOZ-Ac precursor. We find that films deposited from solutions with increased zirconium hydrolysis demonstrated a high overall inorganic network connectivity resulting in a hybrid organic–inorganic film with a highly cross-linked molecular network. As a result, these films are capable of *inhibiting* moisture-assisted

Received: January 12, 2015
Accepted: March 9, 2015
Published: March 9, 2015

DOI: 10.1021/acsami.5b00344
ACS Appl. Mater. Interfaces 2015, 7, 6812−6818

degradation between a silicon substrate and an epoxy layer while improving the adhesion of the bare epoxy/Si interface by threefold.

2. RESULTS AND DISCUSSION

2.1. Fracture in Moist and Inert Environments. The debond growth rates, da/dt, over the range from 1×10^{-4} to 1×10^{-9} m/s in hybrid layers (HL) deposited from solutions with varying TPOZ-Ac prehydrolysis times were measured as a function of the applied debond driving force G, using a thin-film delamination technique at 85% relative humidity (RH) and 25 °C (Figure 1).[3,4,23] A measurement without an HL at the epoxy/Si interface was included for reference. When collecting time-dependent debonding data, the G values at lower debond growth rates of $\sim 1 \times 10^{-9}$ m/s represent threshold G_{th} values, below which crack propagation is presumed to be dormant.[23] Therefore, if the debond driving force does not exceed the threshold values, crack propagation will not occur.

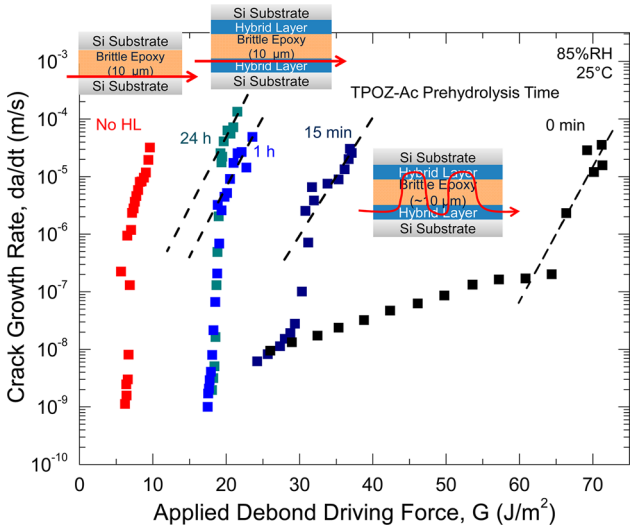

Figure 1. Crack growth rate, da/dt (m/s), as a function of applied debound driving force, G (J/m^2) at a constant temperature of 25 °C and 85% RH is shown for films deposited from solutions with varying TPOZ-Ac prehydrolysis times. The data presented for films deposited from solutions with 15 min and 24 h of TPOZ-Ac prehydrolysis is an average of two collected samples. Dashed lines at the high debond growth rates indicate log−linear fits. The multilayer schematics demonstrate the HL/epoxy film stack used during double cantilever beam testing. The observed fracture paths are represented by the red arrow.

At high debond growth rates, $\sim 1 \times 10^{-4}$ to 1×10^{-5} m/s, the G values varied significantly based on TPOZ-Ac prehydrolysis time; ~70, 35, 25, and 22 J/m^2 for films deposited from solutions with 0 min, 15 min, 1 h, and 24 h of TPOZ-Ac prehydrolysis, respectively. These values are similar to the G_c values measured at room temperature and relative humidity (Figure 2). This is expected because crack growth rates of $\sim 1 \times 10^{-4}$ m/s approach the crack-growth rate regime representative of critical fracture phenomenon. However, despite the difference in the G values at the high debond growth rates, the dependence of G on the debond growth rate was similar across all films with varying TPOZ-Ac prehydrolysis times.

The presence of a strong G dependence on the crack growth rate at $\sim 1 \times 10^{-4}$ to 1×10^{-6} m/s suggests that this crack-growth regime is limited by the rate of a chemical reaction occurring at the crack tip. If the crack growth rate is assumed to be proportional to the rate of a chemical reaction at the crack tip, then

$$\frac{da}{dt} = A' a_{H2O}^{n} \exp\left(\frac{bG}{RT}\right) \quad (1)$$

where A' is a temperature-dependent coefficient, b is an environment-dependent material constant that is directly proportional to the activation volume, R is the universal gas constant, T is the temperature and a_{H2O} is the environmental species activity. Therefore, at a constant temperature, the slope b/RT of the plot of $\ln(da/dt)$ versus G is independent of a_{H2O}.[3,5,23,25−27] The b/RT terms are similar for all of the films (0.53 ± 0.04 m^2 J^{-1}) suggesting the same crack propagation mechanism in all cases.

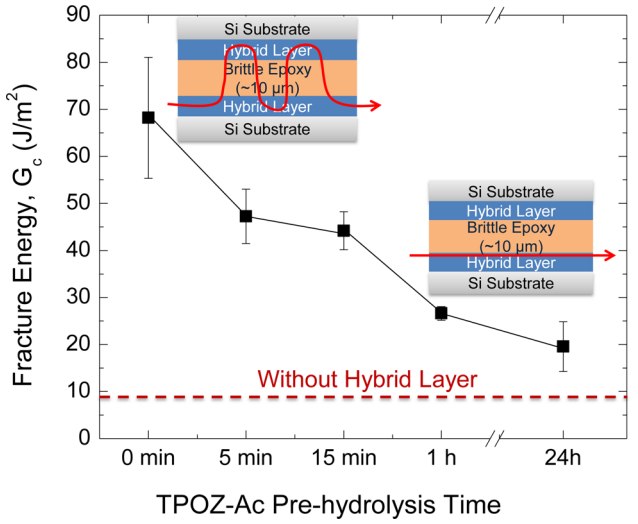

Figure 2. Fracture energy values as a function of TPOZ-Ac prehydrolysis time. The fracture path for films deposited without TPOZ-Ac prehydrolysis was cohesive in the hybrid film and meandered through the epoxy. For films deposited after 24 h of TPOZ-Ac prehydrolysis, the fracture path was also cohesive in the HL but localized and near the adjacent epoxy layer. The multilayer schematics demonstrate the HL/epoxy film stack used during double cantilever beam testing. The observed fracture paths are represented by the red arrow.

The fracture paths (studied via X-ray photoelectron spectroscopy (XPS) and optical microscopy) at high debond growth rates, 1×10^{-4} m/s, were similar to the fracture paths observed for G_c measurements of the HL films. For HLs deposited from solutions without TPOZ-Ac prehydrolysis, the fracture path meandered through the epoxy and failed cohesively within the HL, near the Si substrate. For films deposited from solutions with longer TPOZ-Ac prehydrolysis times, that is, 1 h or 24 h, the fracture path did not meander through the epoxy. However, the fracture was also cohesive in the HL but localized near the epoxy layer rather than the Si substrate.

The trends in fracture paths and measured G_c values of the films deposited from solutions with increasing TPOZ-Ac prehydrolysis are the same as those observed for films deposited from solutions with increasing aging times, which have been previously reported.[15] Furthermore, upon addition of the TPOZ-Ac precursor to water, the solution was heterogeneous and became more homogeneous with increasing TPOZ-Ac hydrolysis time.[15] This suggests that the aging

DOI: 10.1021/acsami.5b00344
ACS Appl. Mater. Interfaces 2015, 7, 6812−6818

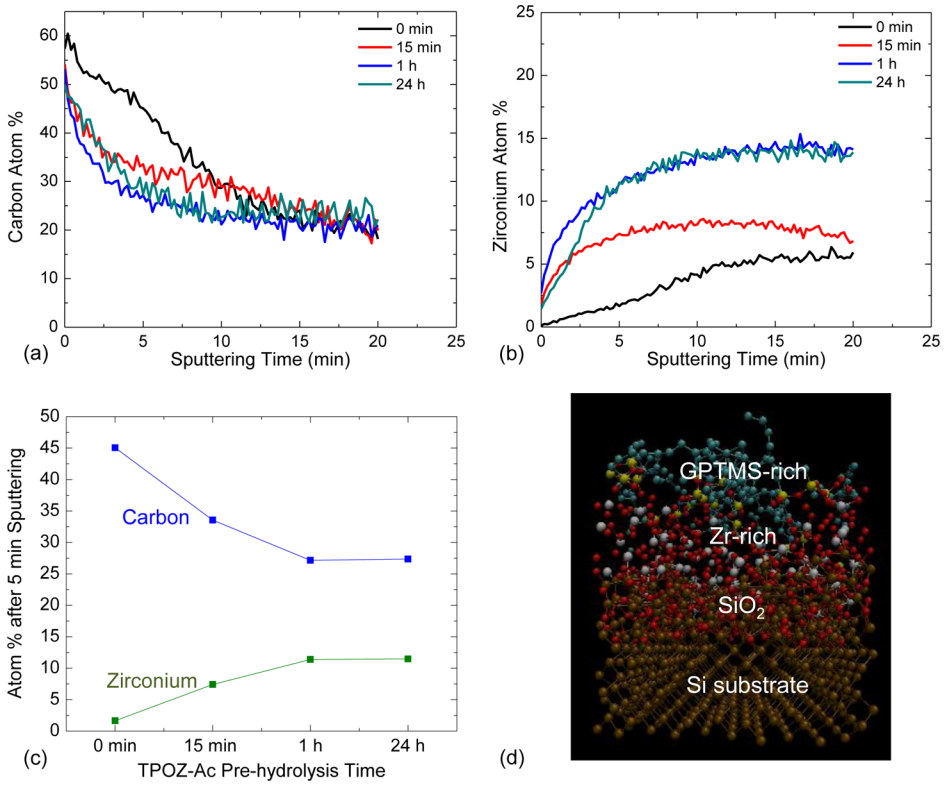

Figure 3. XPS depth profiling of (a) carbon and (b) zirconium content through the thickness of hybrid films deposited from solutions with a varying amount of TPOZ-Ac prehydrolysis time. The data indicate the carbon and zirconium content obtained from sputtering through the film until the hybrid layer/silicon interface was reached. (c) Atom % of carbon and zirconium present in the film after 5 min of sputtering (i.e., within ~10 nm of the film thickness). (d) A schematic of the compositionally graded hybrid film deposited on a silicon substrate derived from conclusions drawn from XPS depth profiling results. Green and yellow atoms represent the carbon and silicon on the GPTMS, respectively. White atoms represent the zirconium, red atoms the oxygen, and brown atoms the silicon from the silicon substrate.

phenomenon, which correlates to an increase in solution homogeneity, is related to the hydrolysis of the TPOZ-Ac species rather than the GPTMS precursor. To further verify this, we performed prehydrolysis studies using the same solution conditions but prehydrolyzing the GPTMS instead, and we did not observe the same trend in both G_c and fracture paths. Therefore, we hypothesize that the degree of the hydrolysis and condensation of the TPOZ-Ac precursor will have a significant impact on the molecular network connectivity and through-thickness film composition.

The difference in the underlying molecular structure with varying TPOZ-Ac hydrolysis and its impact on the resulting adhesive/cohesive properties of the films is highlighted by the time-dependent debonding behavior of the films. Despite the difference in the G values at high debond growth rates, the G_{th} values for all of the hybrid films converge to lower values. For the films deposited from solutions with 1 and 24 h of TPOZ-Ac prehydrolysis, the G_{th} is ~17 J/m^2, which was threefold the G_{th} value for the brittle epoxy/Si interface in the absence of the HL (~5 J/m^2). For the films deposited from solutions with 0 and 15 min of TPOZ-Ac prehydrolysis, we observe an extended debond plateau leading to G_{th} values far below the G values measured at high debond growth rates. We suggest that this G_{th} convergence to low values is due to the crack paths for all of the films being predominantly cohesive in the HL. This result highlights three important aspects of the behavior of these hybrid organic/inorganic films in high humidity environments.

First, we note that the films deposited from solutions with 1 and 24 h of TPOZ-Ac prehydrolysis significantly decreased the moisture sensitivity of the epoxy/Si interface by increasing the G_{th} value threefold. Second, the difference between the G values at high and low growth rates for each film indicates the importance of measuring such time-dependent debonding phenomenon when understanding the sensitivity of a material or interface to moisture. Finally, the difference in the debonding behavior for films deposited with varying TPOZ-Ac prehydrolysis times suggests, as expected, that the underlying molecular structure of the films changes significantly as a function of TPOZ-Ac prehydrolysis time. Therefore, we leveraged chemical characterization techniques such as XPS and Fourier transform infrared spectroscopy (FTIR) to unravel the underlying molecular structure and to understand its impact on the adhesive/cohesive properties of the films in high humidity environments.

2.2. Interfacial and Bulk Film Characterization. We studied the through-thickness composition of the films deposited from solutions with varying TPOZ-Ac hydrolysis time using XPS depth profiling. Figure 3a,b indicates the XPS depth profiles for the carbon (C) and zirconium (Zr) content, respectively, in films deposited from solutions with varying TPOZ-Ac prehydrolysis times. Because of the high carbon content provided by the GPTMS, the C atom % was used as a trace for the organic network in the film, while the Zr atom % was indicative of the inorganic network. The sputtering was done through the entire thickness of the film until the HL/Si interface was reached. Toward the bottom of the film, that is, at sputtering times of 20 min, the C content converged to 20 atom % for all of the films; however, the Zr content varied

DOI: 10.1021/acsami.5b00344
ACS Appl. Mater. Interfaces 2015, 7, 6812−6818

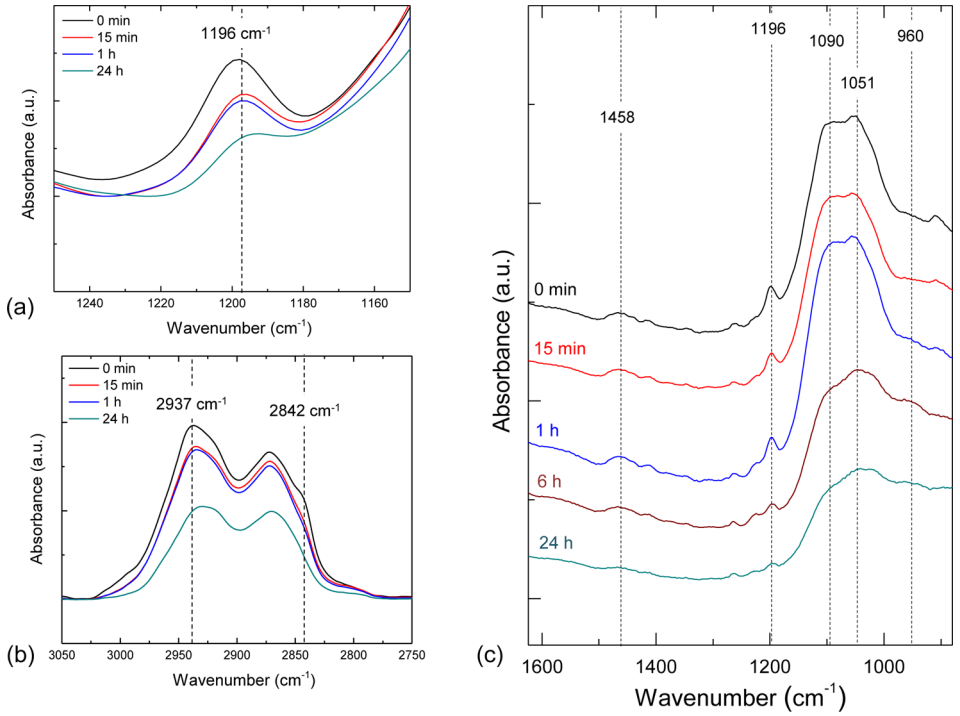

Figure 4. Transmission FTIR of as-deposited films indicating a decrease in the peak intensity at (a) 1196 cm^{-1} and at (b) 2937 and 2842 cm^{-1} with increasing TPOZ-Ac prehydrolysis time. These peaks are attributed to the presence of methoxy ($-OCH_3$) groups in the GPTMS. (c) ATR-FTIR of films deposited with increasing TPOZ-Ac prehydrolysis time. Similar to the transmission FTIR data, a decrease in the peak intensity at 1196 cm^{-1} with increasing TPOZ-Ac prehydrolysis time is also observed in the ATR-FTIR data. Furthermore, the peak at 1090 cm^{-1} is also attributed to Si-OCH_3 groups, which decreases in intensity with increasing prehydrolysis time. A decrease in the intensity and broadening of the peak at 1051 cm^{-1} with increasing TPOZ-Ac prehydrolysis time is indicative of decreasing Si−O−Si bonding. Finally, the peak at 1458 cm^{-1} is attributed to acetate-bound zirconium groups, and that at 960 cm^{-1} is attributed to Zr−O−Si bonds.

significantly depending on the TPOZ-Ac prehydrolysis time. The Zr content toward the bottom of the film increased dramatically, from ∼5 atom % for films without TPOZ-Ac prehydrolysis to ∼15 atom % for films with 24 h of TPOZ-Ac prehydrolysis.

The chemical composition near the top of the films also varied significantly depending on the degree of hydrolysis of the TPOZ-Ac precursor. As the TPOZ-Ac prehydrolysis time increased, we observed a steady decrease in the C content toward the top of the film, that is, at sputtering times of 5 min, which correspond to ∼10 nm into the film, from ∼45 atom % with no TPOZ-Ac prehydrolysis to ∼25 atom % for the longer TPOZ-Ac prehydrolysis times. Furthermore, the Zr content near the top of the film also varied dramatically. At the same sputtering time of 5 min, the Zr content steadily increased from 2 to 12 atom % for films deposited without TPOZ-Ac prehydrolysis and with 24 h of TPOZ-Ac prehydrolysis, respectively.

To highlight the difference in the compositionally graded structure of the films, Figure 3c shows the atom % measured after sputtering into the film for 5 min as a function of the TPOZ-Ac prehydrolysis time. As discussed above, the composition gradient decreases significantly with increasing TPOZ-Ac prehydrolysis time. Nevertheless, these XPS depth profiling results suggest that all of the films demonstrate a compositionally graded structure, where the top of the film is organic-rich, while the bottom of the film is zirconium-rich, which is demonstrated in the schematic in Figure 3d.

In the case of films deposited from solutions without TPOZ-Ac prehydrolysis, the TPOZ-Ac species have not had enough time to fully hydrolyze in solution. As a result, when we dip coat the films, only a fraction of the TPOZ-Ac species that was hydrolyzed selectively deposit on the substrate, while the top of the film is enriched with the hydrolyzed GPTMS precursor.[15] Further details of this suggested mechanism have been described elsewhere.[15] When the TPOZ-Ac is prehydrolyzed for longer periods of time, that is, 1 and 24 h, the species become more soluble in solution. This results in the solution transitioning from cloudy to clear after 1 h of hydrolysis time. When the films are deposited from these solutions, the selective deposition effect is no longer achievable, resulting in a film with a more uniform composition through the thickness. It is concluded that the reduction of the compositionally graded structure throughout the thickness of the films is directly related to the increased solubility of the TPOZ-Ac species in solution. These changes in the hybrid molecular structure and network connectivity were also investigated with transmission FTIR and attenuated total-reflectance (ATR) FTIR.

Since the films were all ∼30−50 nm thick, the resulting noise in the transmission FTIR data from the Si substrate inhibited the ability to analyze the entire spectrum. Therefore, ATR-FTIR was used to supplement the results of the FTIR transmission data. We first studied the characteristic absorbance peaks of two primary chemical groups on both the GPTMS and TPOZ-Ac precursors, namely, the silicon-bonded methoxy (Si-OMe) groups on the GPTMS and the acetate-bound Zr groups. The presence of the methoxy groups on the GPTMS and acetate groups on the Zr in the deposited films are both indicative of poor cross-linking of the inorganic network.

DOI: 10.1021/acsami.5b00344
ACS Appl. Mater. Interfaces 2015, 7, 6812−6818

The decrease in the Si-OMe and OMe content with increasing prehydrolysis time is supported by several FTIR peaks. First, we observed a significant decrease in the absorption peak intensity at 1196, 2937, and 2842 cm^{-1} (Figure 4a,b).[28−31] The same trend in the absorption of the peak at 1196 cm^{-1} was also observed in the ATR-FTIR data (Figure 4c). Furthermore, Si-OMe groups are also identified by a strong absorption at 1080−1100 cm^{-1} (Figure 4c).[29] This peak both broadens and decreases in intensity with increasing prehydrolysis time (Figure 4c). Since these Si-OMe groups are associated with the GPTMS, it is suggested that the reduction of these groups in the deposited films with increasing TPOZ-Ac prehydrolysis time is a result of increased connectivity of the Si atom in the GPTMS, forming Zr−O−Si bonds. Interestingly, the peak at 1051 cm^{-1}, associated with Si−O−Si bonding, decreases in intensity with increasing prehydrolysis.[14,32−34] Since the GPTMS hydrolysis time is kept constant for all of the solutions, it suggests that more Si−O−Zr bonds have formed.

We also used more direct evidence of inorganic network connectivity by studying the peak intensity of the Si−O−Zr bond in the deposited films. Unfortunately, the characteristic peak for Zr−O−Zr bonding was difficult to identify due to noise of the spectra at low wavenumbers. We found that the peak at 960 cm^{-1}, which is associated with Zr−O−Si bonding, increased in intensity with increasing TPOZ-Ac prehydrolysis time.[14,35] The increase in Zr incorporation into the network is also evidenced by the decrease of the peak at 1458 cm^{-1}, which correlates to the acetate-bound Zr groups, with increasing TPOZ-Ac prehydrolysis time.[19,36] As anticipated, the acetate groups on the Zr are displaced with increasing prehydrolysis time, resulting in the formation of Zr−OH groups. These can therefore condense with other Zr−OH groups or with Si−OH groups on the GPTMS and increase the inorganic network connectivity of the films.

We have shown that the degree of hydrolysis of the TPOZ-Ac species has a significant effect on both the composition gradient as well as the inorganic network connectivity of the deposited films. Although all of the films have a compositionally graded structure, with a GPTMS-rich region near the top of the film and Zr-rich region near the bottom of the film, the gradient is significantly reduced with increasing TPOZ-Ac prehydrolysis. However, films deposited from solutions with longer TPOZ-Ac prehydrolysis contain a higher degree of inorganic network connectivity than films deposited without TPOZ-Ac prehydrolysis. Leveraging these chemical characterization techniques to draw insight on the tradeoff between composition gradients and inorganic network connectivity with increasing TPOZ-Ac prehydrolysis allowed us to further understand the behavior of the time-dependent debonding studies.

2.3. Effect of Hybrid Molecular Structure on Debond Kinetics. We suggest that the high G values at high growth rates for films deposited from solutions without TPOZ-Ac prehydrolysis are a result of the carbon-rich region near the top of the film, leading to higher cross-linking with an adjacent epoxy. This forces the fracture path to be cohesive within the HL, through the bonds between the inorganic Zr network and the Si substrate before meandering through the epoxy and dissipating energy. On the other hand, the reduced G values at high growth rates for films deposited with increasing TPOZ-Ac prehydrolysis times is a result of the decreased compositionally graded structure. Here, the decrease in the GPTMS content near the top of the film led to localized cohesive failure in the HL near the adjacent epoxy layer.

At intermediate debond growth rates of 1×10^{-7} to 1×10^{-8} m/s, we observed very different behavior for films deposited from solutions with varying TPOZ-Ac prehydrolysis time. For films deposited from solutions without TPOZ-Ac prehydrolysis, we observed a stress-dependent plateau spanning across 40 J/m^2 of debond driving force. Here, the G versus da/dt slope was significantly reduced, meaning that the plateau region exhibited only a weak dependence on G. This plateau was also observed for films deposited from solutions with 15 min of TPOZ-Ac prehydrolysis. Plateaus that are similar in nature to the ones presented in this study are typically associated with a transport-limited crack-growth rate regime where crack growth rates are limited by the diffusion of environmental species ahead of the propagating crack tip. This behavior has been previously reported for polymer/Si interfaces exposed to high humidity environments and has been correlated to the diffusion of moisture through an adjacent organic layer, attacking regions of the interface ahead of the crack tip.[3]

Here, it is possible that the same rate-limiting phenomenon is occurring to give rise to the plateaus, in which water is diffusing into the HL, and displacing weak bonds at the HL/Si substrate interface. As discussed above, in these solution conditions, the precursors hydrolyze for a limited period of time, resulting in low inorganic network connectivity. Therefore, it is possible that this diffusion effect could be a result of low bond density at the HL/Si substrate interface. Since TPOZ-Ac is the primary inorganic network former for this system, increased hydrolysis should also lead to an increase in bond density at the HL/Si interface.

The films deposited from solutions with increasing TPOZ-Ac prehydrolysis did not show a stress-dependent plateau at intermediate growth rates. In this case, the TPOZ-Ac was hydrolyzed for sufficient time to form a dense hybrid organic/inorganic network and a strong bond at the HL/Si interface. This is supported by the observed increase in the zirconium content of the deposited films as well as an increase in the overall inorganic molecular network connectivity. We suggest that this will result in a more tortuous path for moisture diffusion at the HL/Si interface, limiting the continued growth of defects at the interface, ahead of the crack tip.

3. CONCLUSION

These results demonstrate the design of multifunctional hybrid organic/inorganic films that are capable of mitigating moisture-assisted degradation of a Si/epoxy interface. We show that the introduction of such films can increase the adhesion of these interfaces by up to 10-fold in inert environments. To understand the resistance of these hybrid materials to moisture, we leveraged time-dependent debonding studies, which demonstrated a threefold improvement in the G_{th} compared to a Si/epoxy interface in the absence of the films. We found that the differing time-dependent debonding behavior of the films deposited from solutions with varying TPOZ-Ac prehydrolysis times was a direct result of the underlying molecular structure.

We show that without TPOZ-Ac prehydrolysis, films with a GPTMS-rich region near the top of the film were obtained, capable of forming a strong bond with an adjacent epoxy. This caused the fracture path to meander through the epoxy, dissipating energy, and resulting in high adhesion values. On the other hand, increasing the TPOZ-Ac prehydrolysis decreased the composition gradient of the film and resulted in a reduction in adhesion. However, we find that by increasing

DOI: 10.1021/acsami.5b00344
ACS Appl. Mater. Interfaces 2015, 7, 6812−6818

the TPOZ-Ac prehydrolysis, we increase the inorganic network connectivity, which prevented the continued growth of defects at the HL/Si interface. Despite this tradeoff in composition gradient and network connectivity, we show that hybrid organic/inorganic films containing a dense inorganic zirconium network are capable of mitigating moisture-assisted degradation of an epoxy/Si interface.

4. EXPERIMENTAL SECTION

A. Preparation of Sol−Gel Solutions. The metal alkoxide used in this study was tetra-*n*-propoxyzirconium (TPOZ, 70% in *n*-propyl alcohol, Sigma-Aldrich Co.), while the epoxy-functionalized silane was (3-glycidoxypropyl)trimethoxysilane (GPTMS, Sigma-Aldrich). To prevent fast precipitation of ZrO_2 out of solution, the TPOZ was stabilized with 45 wt % glacial acetic acid (GAA, EMD, Gibbstown, NJ) to introduce acetate ligands on the zirconium (TPOZ-Ac), which slowed the hydrolysis.[36,37] All of the sol−gel solutions consisted of 3.75 wt % solids in deionized water with a zirconate/GPTMS molar ratio of 0.7.[14,15] Solutions were prepared according to the prehydrolysis of the TPOZ-Ac precursor. To synthesize films with prehydrolyzed zirconium, the TPOZ-Ac was added to an excess of water and prehydrolyzed for 5 min, 15 min, 1 h, or 24 h. The GPTMS was then added to the solution and stirred at 500 rpm for 5 min. Reference samples, that is, "no pre-hydrolysis" condition, were synthesized by mixing GPTMS and TPOZ-Ac simultaneously into an 80 mL beaker with deionized water and aging for 5 min prior to deposition. Since glacial acetic acid was used to stabilize the TPOZ, the pH of the solution was 3.5.

B. Film Deposition and Curing. Immediately after the 5 min of aging of all the solutions, the stirring was stopped, and films were deposited by dip coating onto substrates (50 × 12.5 × 0.777 mm) of natively oxidized single-crystal [100] silicon. The silicon substrates were submerged in the sol−gel at a rate of 10 mm/s and immediately withdrawn using a rate of 1 mm/s. The films were then thermally cured for 2 h at 120 °C in air.

C. Chemical Characterization. Film thickness was measured with a surface profilometer (Dektak 150). X-ray photoelectron spectroscopy (XPS, PHI 5000 Versaprobe system) using an Al Kα X-ray radiation and C60 sputtering was used to measure the through-thickness composition of the as-deposited films. The molecular structure of the network was studied using both transmission FTIR and ATR-FTIR (Thermo Nicolet Nexus 670). For ATR-FTIR, absorption spectra were measured for the films deposited onto silicon using a single-reflection ATR fixture with a germanium crystal. For all FTIR data, a total of 32 scans were collected at a resolution of 2 cm^{-1}.

D. Mechanical Testing. The fracture energy of each hybrid film was measured in terms of the critical strain energy release rate G_c, using double cantilever beam (DCB) specimens. The double cantilever beam (DCB) test geometry is a well-established method for measuring the critical strain energy release rate of thin-film structures and interfaces.[21] In this study, DCB test specimens were fabricated by bonding together two sol−gel coated silicon substrate pieces with a 10 μm thick bondline of a highly cross-linked brittle bisphenol-F resin to form a symmetric sandwich test structure. The specimens were then cured at 100 °C for 2 h in air. Subsequently, the DCB specimens were loaded under displacement control at a rate of 0.2 μm/s, from which a load versus displacement curve was recorded. All G_c testing was carried out in laboratory air environment, which remained constant at 25 °C and ∼40−45% RH. Equation 1 below was used to calculate G_c, where P_c is the critical load at which crack growth occurs, a is the crack length, E is the plane strain elastic modulus, and the specimen dimensions are width B and beam-thickness h.[38]

$$G_c = \frac{12P_c^2a^2}{B^2E'h^3}\left(1 + 0.64\frac{h}{a}\right)^2 \quad (1a)$$

To study the time-dependent debonding of the hybrid layer films, the entire system was placed in a controlled environment at constant temperature (±1 °C) and RH (±2% RH) after a 12 h equilibration period. The general method to measure the debond growth rate da/dt as a function of the applied debond driving force G involves loading techniques and compliance methods that have been described elsewhere.[21] To briefly describe, the fracture specimens were loaded to a predetermined load at which the displacement was fixed. The rate of load relaxation that results from crack extension was measured to calculate the crack growth velocity. Subcritical crack growth velocities were characterized as a function of the applied debond driving force G over the range of ∼1×10^{-4} to 1×10^{-9} m/s to produce a characteristic da/dt versus G curve. These measurements were conducted at 85% RH and 25 °C. After DCB testing, surface XPS scans (0−1000 eV) with optical microscopy of the fracture surfaces was used to determine the debond pathway in the film structures.

AUTHOR INFORMATION

Corresponding Authors

*E-mail: gdubois@us.ibm.com. (G.D.)
*E-mail: dauskardt@stanford.edu. (R.H.D.)

Funding

This work was supported by the Air Force Office of Scientific Research Grant No. FA9550−12−1−0120.

Notes

The authors declare no competing financial interest.

ACKNOWLEDGMENTS

The authors would like to thank J. A. Burg for his molecular-dynamics simulations.

REFERENCES

(1) Guyer, E. P.; Dauskardt, R. H. Fracture of Nanoporous Thin-Film Glasses. *Nat. Mater.* **2004**, *3* (1), 53−57.
(2) Guyer, E. P.; Dauskardt, R. H. Effect of Solution pH on the Accelerated Cracking of Nanoporous Thin-Film Glasses. *J. Mater. Res.* **2005**, *20* (3), 680−687.
(3) Sharratt, B. M.; Wang, L. C.; Dauskardt, R. H. Anomalous Debonding Behavior of a Polymer/Inorganic Interface. *Acta Mater.* **2007**, *55* (10), 3601−3609.
(4) Wiederhorn, S. M.; Fuller, E. R.; Thomson, R. Micromechanisms of Crack Growth in Ceramics and Glasses in Corrosive Environments. *Met. Sci.* **1980**, *14* (8−9), 450−458.
(5) Wiederhorn, S. M.; Freiman, S. W.; Fuller, E. R.; Simmons, C. J. Effects of Water and Other Dielectrics on Crack-Growth. *J. Mater. Sci.* **1982**, *17* (12), 3460−3478.
(6) Lawn, B. R. An Atomistic Model of Kinetic Crack Growth in Brittle Solids. *J. Mater. Sci.* **1975**, *10* (3), 469−480.
(7) Novoa, F. D.; Miller, D. C.; Dauskardt, R. H. Environmental Mechanisms of Debonding in Photovoltaic Backsheets. *Sol. Energy Mater. Sol. Cells* **2014**, *120*, 87−93.
(8) Lewis, J. S.; Weaver, M. S. Thin-Film Permeation-Barrier Technology for Flexible Organic Light-Emitting Devices. *IEEE J. Sel. Top. Quantum Electron.* **2004**, *10* (1), 45−57.

DOI: 10.1021/acsami.5b00344
ACS Appl. Mater. Interfaces 2015, 7, 6812−6818

(9) Snodgrass, J. M.; Pantelidis, D.; Jenkins, M. L.; Bravman, J. C.; Dauskardt, R. H. Subcritical Debonding of Polymer/Silica Interfaces under Monotonic and Cyclic Loading. *Acta Mater.* **2002**, *50* (9), 2395−2411.
(10) Mammeri, F.; Le Bourhis, E.; Rozes, L.; Sanchez, C. Mechanical Properties of Hybrid Organic-Inorganic Materials. *J. Mater. Chem.* **2005**, *15* (35−36), 3787−3811.
(11) Sanchez, C.; Julian, B.; Belleville, P.; Popall, M. Applications of Hybrid Organic-Inorganic Nanocomposites. *J. Mater. Chem.* **2005**, *15* (35−36), 3559−3592.
(12) Wu, K. H.; Li, M. C.; Chang, T. C.; Yang, C. C. Characterization and Corrosion Resistance of Organically Modified Silicate/MO2 (M = Zr, Ti, or Ce) Hybrid Coatings on a 6061-T6 Aluminum Alloy. *J. Polym. Sci, Part A: Polym. Chem.* **2006**, *44* (1), 335−342.
(13) Liu, J.; Chaudhury, M. K.; Berry, D. H.; Seebergh, J. E.; Osborne, J. H.; Blohowiak, K. Y. Effect of Surface Morphology on Crack Growth at a Sol-Gel Reinforced Epoxy/Aluminum Interface. *J. Adhes.* **2006**, *82* (5), 487−516.
(14) Oliver, M. S.; Blohowiak, K. Y.; Dauskardt, R. H. Molecular Structure and Fracture Properties of ZrO(X)/Epoxysilane Hybrid Films. *J. Sol—Gel Sci. Technol.* **2010**, *55* (3), 360−368.
(15) Giachino, M.; Dubois, G.; Dauskardt, R. H. Heterogeneous Solution Deposition of High-Performance Adhesive Hybrid Films. *ACS Appl. Mater. Interfaces* **2013**, *5* (20), 9891−9895.
(16) Sanchez, C.; Ribot, F.; Lebeau, B. Molecular Design of Hybrid Organic-Inorganic Nanocomposites Synthesized via Sol-Gel Chemistry. *J. Mater. Chem.* **1999**, *9* (1), 35−44.
(17) Blohowiak, K. Y.; Osborne, J. H.; Krienke, K. A. *Sol Coating of Metals*. U.S. Patent 5,849,110, December 15, 1998.
(18) Yang, J.; Dauskardt, R. H. Hybrid Coupling Layers for Bulk Metallic Glass Adhesion. *J. Mater. Res.* **2013**, *28* (22), 3164−3169.
(19) Voevodin, N. N.; Grebasch, N. T.; Soto, W. S.; Kasten, L. S.; Grant, J. T.; Arnold, F. E.; Donley, M. S. An Organically Modified Zirconate Film as a Corrosion-Resistant Treatment for Aluminum 2024-T3. *Prog. Org. Coat.* **2001**, *41* (4), 287−293.
(20) Le Blanc, L.; Campazzi, E.; Savigne, P. Sol for Sol-Gel Process Coating of a Surface and Coating Method by Sol-Gel Processing. U.S. Patent 0148711A1, June 11, 2009.
(21) Dauskardt, R.; Lane, M.; Ma, Q.; Krishna, N. Adhesion and Debonding of Multi-Layer Thin Film Structures. *Eng. Fract. Mech.* **1998**, *61* (1), 141−162.
(22) Dupont, S. R.; Novoa, F.; Voroshazi, E.; Dauskardt, R. H. Decohesion Kinetics of PEDOT:PSS Conducting Polymer Films. *Adv. Funct. Mater.* **2014**, *24* (9), 1325−1332.
(23) Kook, S. Y.; Dauskardt, R. H. Moisture-Assisted Subcritical Debonding of a Polymer/Metal Interface. *J. Appl. Phys.* **2002**, *91* (3), 1293−1303.
(24) Lane, M. W.; Snodgrass, J. M.; Dauskardt, R. H. Environmental Effects on Interfacial Adhesion. *Microelectron. Reliab.* **2001**, *41* (9−10), 1615−1624.
(25) Bhatnagar, A.; Hoffman, M. J.; Dauskardt, R. H. Fracture and Subcritical Crack-Growth Behavior of Y-Si-Al-O-N Glasses and Si_3N_4 ceramics. *J. Am. Ceram. Soc.* **2000**, *83* (3), 585−596.
(26) Crichton, S. N.; Tomozawa, M.; Hayden, J. S.; Suratwala, T. I.; Campbell, J. H. Subcritical Crack Growth in a Phosphate Laser Glass. *J. Am. Ceram. Soc.* **1999**, *82* (11), 3097−3104.
(27) Michalske, T. A.; Bunker, B. C. A Chemical-Kinetics Model for Glass Fracture. *J. Am. Ceram. Soc.* **1993**, *76* (10), 2613−2618.
(28) Smith, A. L. Infrared Spectra-Structure Correlations for Organosilicon Compounds. *Spectrochim. Acta* **1960**, *16* (1−2), 87−105.
(29) Smith, B. C. *Infrared Spectral Interpretation: A Systematic Approach;* CRC Press LLC: Boca Raton, FL, 1999.
(30) Anderson, D. R. *Analysis of Silicones;* Wiley-Interscience: New York, 1974.
(31) Degen, I. A. Detection of the Methoxyl Group by Infrared Spectroscopy. *Appl. Spectrosc.* **1968**, *22* (3), 164−166.
(32) Liu, W.-C.; Yang, C.-C.; Chen, W.-C.; Dai, B.-T.; Tsai, M.-S. The Structural Transformation and Properties of Spin-on Poly(silsesquioxane) Films by Thermal Curing. *J. Non-Cryst. Solids* **2002**, *311* (3), 233−240.
(33) Park, E. S.; Ro, H. W.; Nguyen, C. V.; Jaffe, R. L.; Yoon, D. Y. Infrared Spectroscopy Study of Microstructures of Poly(silsesquioxane)s. *Chem. Mater.* **2008**, *20* (4), 1548−1554.
(34) Cui, L.; Ranade, A. N.; Matos, M. A.; Pingree, L. S.; Frot, T. J.; Dubois, G.; Dauskardt, R. H. Atmospheric Plasma Deposited Dense Silica Coatings on Plastics. *ACS Appl. Mater. Interfaces* **2012**, *4* (12), 6587−6598.
(35) Armelao, L.; Gross, S.; Muller, K.; Pace, G.; Tondello, E.; Tsetsgee, O.; Zattin, A. Structural Evolution upon Thermal Heating of Nanostructured Inorganic-Organic Hybrid Materials to Binary Oxides MO2-SiO2 (M = Hf, Zr) as Evaluated by Solid-State NMR and FTIR Spectroscopy. *Chem. Mater.* **2006**, *18* (25), 6019−6030.
(36) Hayashi, H.; Suzuki, H.; Kaneko, S. Effect of Chemical Modification on Hydrolysis and Condensation Reaction of Zirconium Alkoxide. *J. Sol—Gel Sci. Technol.* **1998**, *12* (2), 87−94.
(37) Yi, G. H.; Sayer, M. An Acetic Acid/Water Based Sol-Gel PZT Process 0.1. Modification of Zr and Ti alkoxides with Acetic Acid. *J. Sol—Gel Sci. Technol.* **1996**, *6* (1), 65−74.
(38) Kanninen, M. F. Augmented Double Cantilever Beam Model for Studying Crack-Propagation and Arrest. *Int. J. Fract.* **1973**, *9* (1), 83−92.

DOI: 10.1021/acsami.5b00344
ACS Appl. Mater. Interfaces 2015, 7, 6812−6818